Aerogel

Subjects: Materials Science, Composites | Nanoscience & Nanotechnology

Contributor: Lei Zhai

Aerogels are one of the most interesting materials of the 21st century owing to their high porosity, low density, and large available surface area. Historically, aerogels have been used for highly efficient insulation and niche applications, such as interstellar particle capture. Recently, aerogels have made their way into the composite universe.

Keywords: aerogel ; nanocomposites ; aerogel composites

1. Introduction

Aerogels have become one of the most exciting materials of the 21st century. The unique processing strategy produces materials with extremely high porosities and low densities, high specific surface areas, high dielectric strengths, and low thermal conductivities [1][2]. These properties have made aerogels novel and intriguing materials for applications in aerospace, energy generation and storage, biomedical devices and implants, sensors, and coatings [2]. Since the introduction of the silica aerogel by Kistler in the 1930s, aerogels have been made out of a variety of materials including metal oxides, chalcogenides, biopolymers, and resins to name a few. More recently, aerogels have entered the realm of nanotechnology, incorporating a variety of nanomaterials into the aerogel matrix and using such materials to create composite aerogels.

While an aerogel's network contains pores with diameters on the order of nanometers, incorporating nanomaterials into an aerogel has further enhanced the functional properties of the aerogels. Since this first use of carbon nanomaterials in the production of an aerogel structure, the utilization of a variety of nanomaterials for the development of high-performance aerogel structures has grown exponentially. For example, carbon nanomaterials such as carbon nanotubes, graphene, and carbon nanofibers have been incorporated into aerogels to improve the electrical conductivity and performance for applications such as supercapacitors, sensors, and batteries [1][3]. In other earlier works, metal chalcogenide nanoparticles were used as quantum dots to create semiconductor aerogels for photovoltaic and sensing applications [4]. In another effort, synergistic composites of nanostructured aerogels and metal oxides were fabricated using atomic layer deposition for catalytic membranes and gas sensors [5].

2. Aerogel Fabrication Strategies

The preparation of aerogels typically involves three distinct steps: (1) the sol-gel transition (gelation), (2) the network perfection (aging), and (3) the gel-aerogel transition (drying). Once the desired materials are selected for the fabrication of the aerogel, the precursor materials are dispersed in a liquid (i.e., colloidal dispersion) and allowed to gel, thus forming a continuous network of solid particles throughout the liquid [6]. For some materials, the transition from a colloidal dispersion into a gel happens without the addition of crosslinking materials [7]. For others, crosslinking materials are added to the dispersion to promote the strong interaction of the solid particles in order to form the gel [8][9]. The gelation time depends heavily on a variety of factors such as the chemical composition of the precursor solution, the concentration of the precursor materials and additives, the processing temperature, and the pH [8][10][11][12][13]. Many materials may require additional curing after gelation (i.e., network perfection) in order to strengthen the aerogel network [8][14][15][16][17][18]. Once the gelation is completed, the gel is dried in such a way as to minimize the surface tension within the pores of the solid network. This is typically accomplished through supercritical fluid extraction using supercritical carbon dioxide ($scCO_2$) or freeze-drying (**Figure 1**a,b). More recently, the aerogel fabrication scheme has been revolutionized in order to create 3D-printed aerogels.

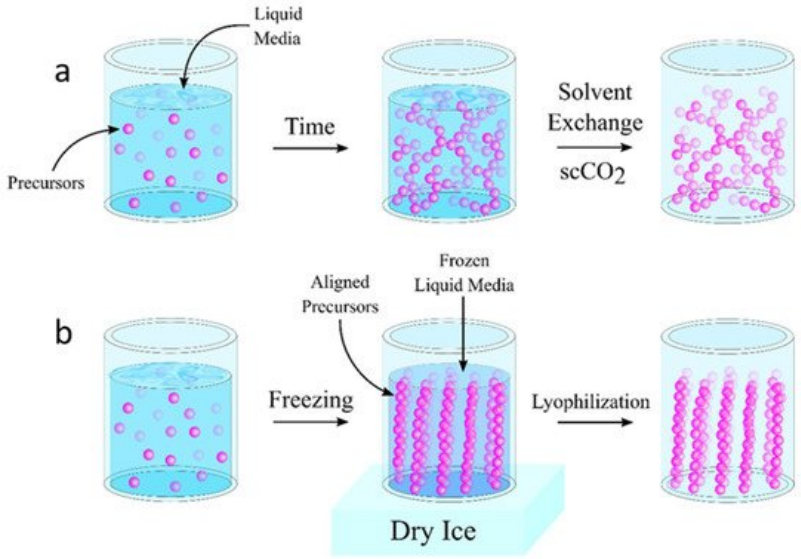

Figure 1. Comparison of aerogel fabrication strategies showing typical transitions into an aerogel. (**a**) shows the supercritical drying process where precursor materials undergo gelation prior to supercritical drying. Often, these processes include a solvent exchange step after gelation to provide better fluids for supercritical drying. (**b**) shows a standard freeze-drying technique where an aqueous solution is frozen and the ice crystal formation dictates the alignment of the precursor materials and thus, the resulting pore structure of the dried aerogel.

2.1. Supercritical Drying

To dry the gel, while preserving the highly porous network of an aerogel, supercritical drying employs the use of the liquid-gas transition that occurs beyond the critical point of a substance (**Figure 1**a and **Figure 2**). By using this liquid-gas transition that avoids crossing the liquid-gas phase boundary, the surface tension that would arise within the pores due to the evaporation of a liquid is eliminated, thereby preventing the collapse of the pores [6]. Through heating and pressurization, the liquid solvent reaches its critical point, at which point the liquid and gas phases become indistinguishable. Past this point, the supercritical fluid is converted into the gaseous phase upon an isothermal de-pressurization. This process results in a phase change without crossing the liquid-gas phase boundary. This method is proven to be excellent at preserving the highly porous nature of the solid network without significant shrinkage or cracking. While other fluids have been reported for the creation of supercritically dried aerogels, $scCO_2$ is the most common substance with a relatively mild supercritical point at 31 °C and 7.4 MPa. CO_2 is also relatively non-toxic, non-flammable, inert, and cost-effective when compared to other fluids, such as methanol or ethanol [19]. While being a highly effective method for producing aerogels, supercritical drying takes several days, requires specialized equipment, and presents significant safety hazards due to its high-pressure operation.

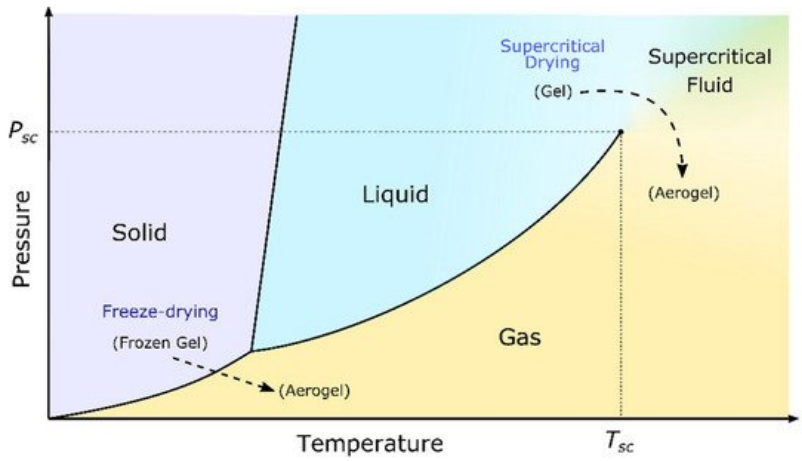

Figure 2. A typical phase diagram for pure compounds. Two methods are shown for the gel to aerogel transition, indicated by I → II. The solid-gas transition depicts the transition from a frozen gel (I) to the dried porous gel (II) during freeze-drying. The transition from a liquid to gas during supercritical drying requires a rise in temperature and pressure (curved arrow from I → II) to avoid crossing the liquid-gas phase boundary. This pass into the supercritical region eliminates surface tension and capillary forces.

2.2. Freeze-Drying

Freeze-drying, also known as freeze-casting or ice-templating, offers an alternative to the high temperature and high-pressure requirements of supercritical drying. Additionally, freeze-drying offers more control of the solid structure development by controlling the ice crystal growth during freezing (**Figure 1**b) [20][21][22][23]. In this method, a colloidal dispersion of the aerogel precursors is frozen, with the liquid component freezing into different morphologies depending on a variety of factors such as the precursor concentration, type of liquid, temperature of freezing, and freezing container [21][22][23]. As this liquid freezes, the solid precursor molecules are forced into the spaces between the growing crystals. Once completely frozen, the frozen liquid is sublimed into a gas through lyophilization, which removes much of the capillary forces, as was observed in supercritical drying (**Figure 2**) [24][25]. Though typically classified as a “cryogel”, aerogels produced through freeze-drying often experience some shrinkage and cracking while also producing a non-homogenous aerogel framework [6].

2.3. 3D Printing

The three-dimensional printing (3DP) of aerogels is revolutionizing the field by enabling a fast and accurate fabrication of complex 3D porous structures, thereby introducing new functionalities, lower costs, and higher reliability in aerogel manufacturing [26][27]. 3DP, in general, is a type of additive manufacturing technique that builds 3D objects through a layer-by-layer growth process [28][29]. This technique makes it possible to fabricate highly customizable and complex structures for many industrial sectors in significantly reduced times while using a variety of materials such as polymers, ceramics, and metals [27][29]. The 3DP of aerogels is considered a hybrid fabrication technique to produce extremely lightweight 3D structures, employing new depositional strategies for the creation of the 3D gel constructs while utilizing the common drying methods of supercritical drying and freeze-drying, as discussed previously.

3DP of aerogel techniques are categorized depending on the sol-gel transitions during the printing process. These categories include: (1) direct ink writing (DIW), where a gel is formed prior to printing [30]; (2) stereolithography (SLA), where the sol-gel transition occurs during printing [31]; and (3) inkjet printing (IJP), where the sol-gel transition occurs after printing (**Figure 3**) [32]. SLA is a technique that prints 3D structures using photocurable materials through a process called photopolymerization, in which polymer layers solidify upon exposure to specific laser wavelengths (**Figure 3**a). IJP is a non-contact, droplet-based material deposition process, with the potential to be modified to deposit photocurable materials to achieve patterning with high resolution (**Figure 3**b). DIW is an extrusion-based printing technique that involves the deposition of continuous ink filaments, in a layer-by-layer fashion, to realize the 3D constructs (**Figure 3**c).

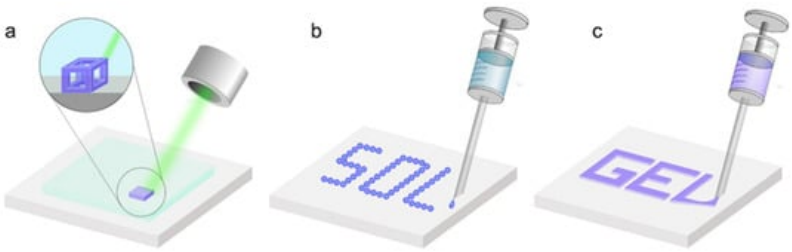

Figure 3. Schematic depiction of the three main 3D-printing techniques employed for the fabrication of aerogels. (**a**) Stereolithography, where a laser is used to transform the sol to a gel during the printing process; (**b**) ink-jet printing, where a solution is printed into its desired structure prior to observing gelation; and (**c**) direct ink writing, where the gel is formed prior to printing and the gel is extruded in order to achieve the desired structure.

3. Applications

Combining the functionalities introduced by nanoscale materials with large surface area of aerogels opens many applications in environment remediation, energy storage, drug delivery and more.

3.1. Environmental Remediation

Porous Sorbents

The large surface area, high porosity, and light weight make aerogels promising sorbent materials. For example, aerogels have been used for environmental remediation to remove spilled oil, organic compounds and heavy metal ions [33]. The wetting properties of aerogels are important in achieving optimal adsorption performance. From this perspective, hydrophobic sorbent materials are of intense interest for application in absorbing hydrocarbons (**Table 1**). In one study, hydrophobic composite aerogels were fabricated from polysilsequioxane-containing phenylene and hexylene-bridge

groups through the polymerization of the polysilsequioxane followed by supercritical drying [34]. The incorporation of the phenylene and hexylene-bridged groups increased the crosslinking density and the molecular weight of the composite aerogel, leading to a significant improvement in the mechanical properties of the aerogel. Additionally, a higher condensation rate of the hexylene-bridged groups produced a more hydrophobic aerogel (contact angle 115°) than the phenylene-bridges (92°). For example, a resorcinol-furfural/silicone hybrid aerogel was fabricated through a facile pressure-drying system at room temperature [35]. In this study, carbon nanotubes were used as a reinforcement material and a trimethylethoxysilane (TMES) solution was used as a surface modifier to increase the hydrophobicity of the aerogel. The TMES replaced the surface hydroxyl groups on the aerogel with stable $–OSi(CH_3)_3$ groups. By doing this, the contact angle increased from 108° to 135°. The highest contact angle was obtained when the ratio of TMES: hexane was 8:1. Another study proposed an interesting method to obtain hydrophobic aerogels through modifying silica gel networks with silylating agent dimethoxy-methyl (3,3,3-trifluoropropyl) silane [36]. The aerogels were synthesized from tetraethoxy silane (TEOS) using a two-step sol-gel process followed by a supercritical drying with CO_2. Duan et al. observed that adding silylating agent to the already produced TEOS gels achieved better results, with the contact angle increasing from 27.5 ± 0.3° to 142.2 ± 0.8°. The addition of the silylating agent significantly affected the resulting hydrophobicity. After the hydrolysis, the TEOS underwent rapid condensation, and gel formation occurs. If the TEOS and silylating agent molecules co-condensed, many of the hydrophobic groups were not exposed to the particle surface. Allowing the hydrolysis before the addition of silylating agent allowed for more functionalization of the gel network surface. The increase in the contact angle for the post-gelation samples was due to the silylating attachment mainly on the exterior of the gelled TEOS particles. In addition to these method studies, it was shown that by increasing wt.% of silylating agent from 5 to 25, contact angle could be increased from 70.6 ± 0.9° to 154.1 ± 0.5°.

Table 1. Comparison of hydrophobic composite aerogels.

Materials	Contact Angle	Density (g cm^{-3})	Absorption Capacity	Compressibility	Ref.
Cellulose-based aerogel	**140°**	**0.0196**	**35 (g/g)**	**80%**	[37]
Polyvinylpolydimethylsiloxane-based aerogels	**140–157°**	**0.02–0.2**	**1200–1600 (%)**	**-**	[38]
Polymethylsilsesquioxane-silk fibroin aerogel	**135° < θ < 145°**	**0.08–0.23**	**~500–2600 g g^{-1} %**	**80%**	[39]
Clay composite aerogel with water repellent (WDisRep3)	**140°**	**0.109**	**-**	**-**	[40]
Magnetic hydrophobic polymer aerogel	**138°**	**0.01384**	**59 to 136 times more than its original weight**	**-**	[41]
Silica-silylated aerogel	**154°**	**0.135**	**-**	**-**	[36]
Silica-chitosan aerogel	**137°**	**0.062**	**30 g/g**	**-**	[42]
Magnetic polystyrene/graphene aerogel	**142°**	**0.005**	**40 times more than its mass**	**-**	[43]
Natural Cellulose Aerogel (Cotton Source)	**142°**	**-**	**100–140 g/g**	**-**	[35]

A new rapid supercritical extraction process has been reported by Jung et al. to produce hydrophobic and transparent aerogels suitable for window shielding [44]. The hydrophobic character was introduced by adding poly(methylmethacrylate) to a silica gel, resulting in the addition of $–OCH_3$ and $–CH_3$ free radicals onto the surface. A silica solution formed the gel structure with the supply of inert gas pressure. Then it was promoted at supercritical conditions through continuous heating. As mentioned previously, cellulose has been used widely in aerogels; however, the hydrophilicity and inferior mechanical properties of cellulose aerogels limit their applications in absorbing organic contaminants. Yu et al. produced high-performance cellulose aerogels by freeze-casting aqueous suspensions of polyvinyl alcohol and cellulose nanofibrils in the presence of hydrolyzed methyltrimethoxysilane sol [45]. The silanol groups (Si–OH) reacted with hydroxyl groups on PVA and cellulose, as well as condensed among themselves to form a Si–O–Si network, leading to robust hydrophobic aerogels. The aerogel has a high absorption capacity of 45–99 times of their own weights, high oil/water selective sorption, and excellent reusability with absorption retention of more than 84% after 35 absorption–squeezing cycles (**Figure 4**).

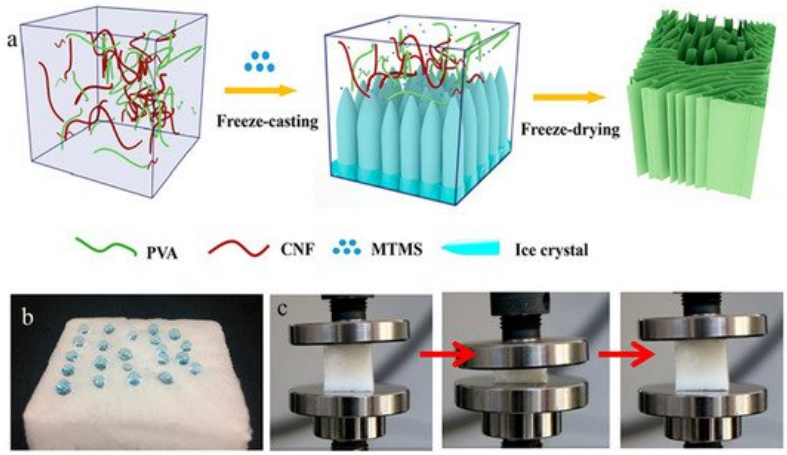

Figure 4. (**a**) A schematic illustration of fabricating hydrophobic cellulose aerogels. (**b**) A picture showing water droplets on the aerogels. (**c**) Pictures showing recovering of an aerogel from compression. Adapted from [45] with permission, copyright the American Chemical Society, 2019.

Commercially available, flexible and mechanically durable fiber-reinforced silica aerogel composites have been evaluated for oil spill cleanup (**Figure 5**) [46]. Thermal Wrap (TW) (6.0 mm thickness, Cabot Corporation, Boston, MA) is a composite of trimethylsilylated silica aerogel particles attached on bicomponent polyester fibers, and Spaceloft (SL) (10 mm thickness, Aspen Aerogels, Northborough, MA, USA) is a composite of a lofty fibrous batting of polyester and glass fibers infiltrated with trimethylsilylated silica aerogel and magnesium hydroxide. As shown in **Figure 5**, both aerogel blankets have hydrophobic silica nanoparticles attaching to fibers, leading to a hydrophobic/oleophilic property. The study indicated that these aerogel composites possessed three important desirable properties for oil spill cleanup: fast oil sorption (3–5 min), reusability (demonstrated over 10 cycles with preserved tensile strength for TW; 380–700 kPa), and recoverability (up to 60% via mechanical extraction).

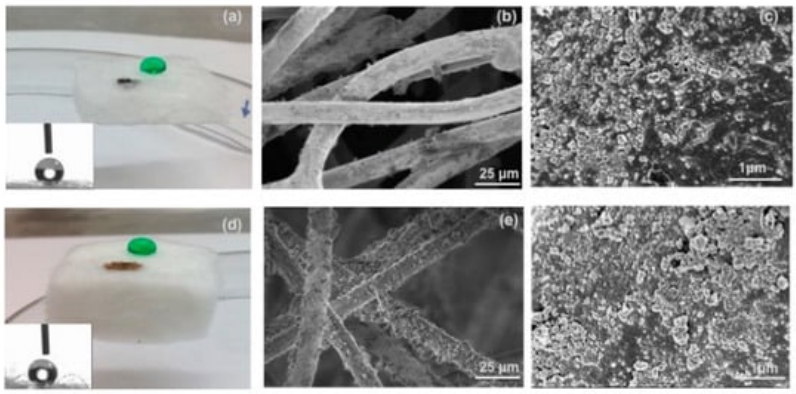

Figure 5. Optical interrogation of aerogel fabrics' gross and fine structure. Image of a dyed-green water droplet and Iraq oil on the surface of (**a**) TW (6 mm thick) and (**d**) SL (10 mm thick). Insets are images from the WCA measurements. Please note that the TW used is thinner than SL. SEM images of the surfaces of (**b** and **c**) TW and (**e** and **f**) SL, where aerogel particles are visible on the fibers in high-resolution. Reprinted from [46] with permission, copyright American Chemical Society, 2016.

3.2. Energy Storage

Over the past decades, great research efforts have been devoted to building high-performance, cost-effective, renewable, and sustainable energy storage devices to meet the need for renewable energy, electric vehicles, and portable electronics. Among many devices developed to address such needs, advanced batteries and supercapacitors are leading this quest. Batteries, owing to their high energy density and ability to supply a constant source of electrical power, dominate the worlds of portable electronics and electric vehicles. This is especially true for lithium-ion type batteries (LIBs) [47]. Supercapacitors, on the other hand, are ideal for short-term energy needs due to their extremely quick and high efficiency charging capabilities, while also being able to operate for a virtually unlimited number of charge-discharge cycles [48][49]. Thus, batteries and supercapacitors are complementary energy storage devices [50].

Improving battery and supercapacitor electrodes is essential to offer higher capacitances and efficiencies, lower the costs, and create more eco-friendly devices. Carbon aerogels have been at the forefront of such research efforts due to carbon's

inherently high surface area, chemical stability, low cost, and eco-friendliness [51]. The hierarchical porous carbon framework in aerogels greatly increases the ability to store electric charge by enabling faster electrolyte ion diffusion rates, creating more active sites for the energy conversion process, and presenting a continuous charge transfer pathway [52]. For batteries, the aerogel structures create space within the electrode to accommodate any volume changes that occur during the charge–discharge cycles that is unavailable in traditional electrode materials [53].

The chemistry, fabrication, and properties of a variety of carbon-based aerogels have been extensively studied for energy storage applications [54][55][56]. While carbon nanotubes, graphene, and graphene derivatives have been used extensively in producing aerogels for energy storage applications [57], bio-based carbon materials are abundant and extremely cost-effective, while offering biodegradability and biocompatibility [58][59], offering flexible, fully disposable electrodes [49][60]. This section aims to provide an overview of the electrochemical performances of graphene and cellulose-based aerogels as LIB and supercapacitor electrodes over the last few years.

3.3. Biomedical Applications

The typical low density, high porosity, and high surface area of aerogels make them suitable for many biomedical applications, including drug delivery, tissue engineering, implantable devices, biomedical imaging, and biosensing [61][62][63][64]. Previously, only silica-based aerogels had been investigated for the use in these applications; however, their poor biodegradability inhibited their use in pharmaceutical and biomedical applications [65][66]. At present, polysaccharides such as starch, alginate, and chitosan are being investigated as biomedical aerogels as they provide low toxicity, biocompatibility, and biodegradability [61].

References

1. Araby, S.; Qiu, A.; Wang, R.; Zhao, Z.; Wang, C.H.; Ma, J. Aerogels based on carbon nanomaterials. J. Mater. Sci. 2016, 51, 9157–9189.
2. Pierre, A.C. History of Aerogels. In Aerogels Handbook. Advances in Sol-Gel Derived Materials and Technologies; Aegerter, M., Leventis, N., Koebel, M., Eds.; Springer: New York, NY, USA, 2011; pp. 3–18.
3. Zhang, M.; Fang, S.; Zakhidov, A.A.; Lee, S.B.; Alieve, A.E.; Williams, C.D.; Atkinson, K.R.; Baughman, R.H. Strong, transparent, multifunctinoal, carbon nanotube sheets. Science 2005, 209, 1215–1220.
4. Mohanan, J.L.; Arachchige, I.U.; Brock, S.L. Porous semiconductor chalcogenide aerogels. Science 2005, 307, 397–400.
5. Elam, J.W.; Xiong, G.; Han, C.Y.; Wang, H.H.; Birrell, J.P.; Welp, U.; Hryn, J.N.; Pellin, M.J.; Baumann, T.F.; Poco, J.F.; et al. Atomic layer deposition for the conformal coating of nanoporous materials. J. Nanomater. 2006, 2006, 1–5.
6. Gurav, J.L.; Jung, I.K.; Park, H.H.; Kang, E.S.; Nadargi, D.Y. Silica aerogel: Synthesis and applications. J. Nanomater. 2010, 2010, 23.
7. Hüsing, N.; Schubert, U. Aerogels—Airy Materials: Chemistry, Structure, and Properties. Angew. Chem. Int. Ed. 1998, 37, 22–45.
8. Capadona, L.A.; Meador, M.A.B.; Alunni, A.; Fabrizio, E.F.; Vassilaras, P.; Leventis, N. Flexible, low-density polymer crosslinked silica aerogels. Polymer 2006, 47, 5754–5761.
9. Leventis, N.; Lu, H. Polymer-Crosslinked Aerogels. In Aerogels Handbook. Advances in Sol-Gel Derived Materials and Technologies; Aegerter, M., Leventis, N., Koebel, M., Eds.; Springer: New York, NY, USA, 2011; pp. 251–285.
10. Hench, L.L.; West, J.K. The sol-gel process. Chem. Rev. 1990, 90, 33–72.
11. Mulik, S.; Sotiriou-leventis, C.; Leventis, N. Time-Efficient Acid-Catalyzed Synthesis of Resorcinol—Formaldehyde Aerogels. Chem. Mater. 2007, 19, 6138–6144.
12. Zhang, J.; Cao, Y.; Feng, J.; Wu, P. Graphene-oxide-sheet-induced gelation of cellulose and promoted mechanical properties of composite aerogels. J. Phys. Chem. C 2012, 116, 8063–8068.
13. Hdach, H.; Woignier, T.; Phalippou, J.; Scherer, G.W. Effect of aging and pH on the modulus of aerogels. J. Non-Cryst. Solids 1990, 121, 202–205.
14. Einarsrud, M.; Nilsen, E.; Rigacci, A.; Pajonk, G.M.; Buathier, S. Strengthening of silica gels and aerogels by washing and aging processes. J. Non-Cryst. Solids 2001, 285, 1–7.
15. Soleimani Dorcheh, A.; Abbasi, M.H. Silica aerogel; synthesis, properties and characterization. J. Mater. Process. Technol. 2008, 199, 10–26.

16. Hæreid, S.; Anderson, J.; Einarsrud, M.A.; Hua, D.W.; Smith, D.M. Thermal and temporal aging of TMOS-based aeroge l precursors in water. J. Non-Cryst. Solids 1995, 185, 221–226.

17. Omranpour, H.; Motahari, S. Effects of processing conditions on silica aerogel during aging: Role of solvent, time and t emperature. J. Non-Cryst. Solids 2013, 379, 7–11.

18. Cheng, C.-P.; Iacobucci, P.A. Inorganic Oxide Aerogels and Their Preparation. U.S. Patent 4,717,708, 5 January 1988.

19. Beckman, E.J. Supercritical or near-critical CO2 in green chemical synthesis and processing. J. Supercrit. Fluids 2004, 28, 121–191.

20. Jin, H.; Nishiyama, Y.; Wada, M.; Kuga, S. Nanofibrillar cellulose aerogels. Colloids Surfaces A Physicochem. Eng. Asp. 2004, 240, 63–67.

21. Jiménez-Saelices, C.; Seantier, B.; Cathala, B.; Grohens, Y. Effect of freeze-drying parameters on the microstructure a nd thermal insulating properties of nanofibrillated cellulose aerogels. J. Sol-Gel Sci. Technol. 2017, 84, 475–485.

22. Wang, C.; Chen, X.; Wang, B.; Huang, M.; Wang, B.; Jiang, Y.; Ruoff, R.S. Freeze-Casting Produces a Graphene Oxid e Aerogel with a Radial and Centrosymmetric Structure. ACS Nano 2018, 12, 5816–5825.

23. Simon-Herrero, C.; Caminero-Huertas, S.; Romero, A.; Valverde, J.L.; Sanchez-Silva, L. Effects of freeze-drying conditi ons on aerogel properties. J. Mater. Sci. 2016, 51, 8977–8985.

24. Deville, S. Ice-templating, freeze casting: Beyond materials processing. J. Mater. Res. 2013, 28, 2202–2219.

25. Deville, S. The lure of ice-templating: Recent trends and opportunities for porous materials. Scr. Mater. 2018, 147, 119–124.

26. Zhang, Q.; Zhang, F.; Xu, X.; Zhou, C.; Lin, D. Three-dimensional printing hollow polymer template-mediated graphene lattices with tailorable architectures and multifunctinoal properties. ACS Nano 2018, 12, 1096–1106.

27. Tang, X.; Zhu, C.; Cheng, D.; Zhou, H.; Liu, X.; Xie, P.; Zhao, Q.; Zhang, D.; Fan, T. Architectured leaf-inspired Ni0.33C o0.66S2/graphene aerogels via 3D printing for high-performance energy storage. Adv. Funct. Mater. 2018, 28, 180505 7.

28. Ambrosi, A.; Pumera, M. 3D-printing technologies for electrochemical applications. Chem. Soc. Rev. 2016, 45, 2740–2 755.

29. Zhu, C.; Liu, T.; Qian, F.; Chen, W.; Chandrasekara, S.; Yao, B.; Song, Y.; Duoss, E.B.; Kuntz, J.D.; Spadaccini, C.M.; e t al. 3D printed functional nanomaterials for electrochemical energy storage. Nano Today 2017, 15, 107–120.

30. Farahani, R.D.; Dubé, M.; Therriault, D. Three-Dimensional Printing of Multifunctional Nanocomposites: Manufacturing Techniques and Applications. Adv. Mater. 2016, 28, 5794–5821.

31. Dizon, J.R.C.; Espera, A.H.; Chen, Q.; Advincula, R.C. Mechanical characterization of 3D-printed polymers. Addit. Man uf. 2018, 20, 44–67.

32. Zhang, F.; Wei, M.; Viswanathan, V.V.; Swart, B.; Shao, Y.; Wu, G.; Zhou, C. 3D printing technologies for electrochemic al energy storage. Nano Energy 2017, 40, 418–431.

33. Maleki, H. Recent advances in aerogels for environmental remediation applications: A review. Chem. Eng. J. 2016, 30 0, 98–118.

34. Boday, D.J.; Stover, R.J.; Muriithi, B.; Loy, D.A. Strong, low density, hexylene- and phenylene-bridged polysilsesquioxa ne aerogel-polycyanoacrylate composites. J. Mater. Sci. 2011, 46, 6371–6377.

35. Cheng, H.; Gu, B.; Pennefather, M.P.; Nguyen, T.X.; Phan-Thien, N.; Duong, H.M. Cotton aerogels and cotton-cellulose aerogels from environmental waste for oil spillage cleanup. Mater. Des. 2017, 130, 452–458.

36. Duan, Y.; Jana, S.C.; Lama, B.; Espe, M.P. Hydrophobic silica aerogels by silylation. J. Non-Cryst. Solids 2016, 437, 26 –33.

37. Li, R.; Li, A.; Zheng, T.; Lu, L.; Gao, Y. Hydrophobic and flexible cellulose aerogel as an efficeint, green and resuable io n sorbent. RSC Adv. 2015, 5, 82027–82033.

38. Zu, G.; Kanamori, K.; Maeno, A.; Kaji, H.; Nakanishi, K. Superflexible Multifunctional Polyvinylpolydimethylsiloxane-Bas ed Aerogels as Efficient Absorbents, Thermal Superinsulators, and Strain Sensors. Angew. Chem. Int. Ed. 2018, 57, 97 22–9727.

39. Maleki, H.; Whitmore, L.; Hüsing, N. Novel multifunctional polymethylsilsesquioxane-silk fibroin aerogel hybrids for envi ronmental and thermal insulation applications. J. Mater. Chem. A 2018, 6, 12598–12612.

40. Madyan, O.A.; Fan, M. Hydrophobic clay aerogel composites through the implantation of environmentally friendly water -repellent agents. Macromolecules 2018, 51, 10113–10120.

41. Xu, Z.; Jiang, X.; Zhou, H.; Li, J. Preparation of magnetic hydrophobic polyvinyl alcohol (PVA)-cellulose nanofiber (CNF) aerogels as effective oil absorbents. Cellulose 2018, 25, 1217–1227.

42. Ma, Q.; Liu, Y.; Dong, Z.; Wang, J.; Hou, X. Hydrophobic and nanoporous chitosan-silica composite aerogels for oil absorption. J. Appl. Polym. Sci. 2015, 132, 1–11.

43. Zhou, S.; Jiang, W.; Wang, T.; Lu, Y. Highly Hydrophobic, Compressible, and Magnetic Polystyrene/Fe3O4 Graphene Aerogel Composite for Oil-Water Separation. Ind. Eng. Chem. Res. 2015, 54, 5460–5467.

44. Jung, H.N.R.; Lee, Y.K.; Parale, V.G.; Cho, H.H.; Mahadik, D.B.; Park, H.H. Hydrophobic silica composite aerogels using poly(methyl methacrylate) by rapid supercritical extraction process. J. Sol-Gel Sci. Technol. 2017, 83, 692–697.

45. Zhang, X.; Wang, H.; Cai, Z.; Yan, N.; Liu, M.; Yu, Y. Highly compressible and hydrophobic anisotropic aerogels for selective oil/organic solvent absorption. ACS Sustain. Chem. Eng. 2019, 7, 332–340.

46. Karatum, O.; Steiner, S.A.; Griffin, J.S.; Shi, W.; Plata, D.L. Flexible, Mechanically Durable Aerogel Composites for Oil Capture and Recovery. ACS Appl. Mater. Interfaces 2016, 8, 215–224.

47. Aghajamali, M.; Xie, H.; Javadi, M.; Kalisvaart, W.P.; Buriak, J.M.; Veinot, J.G.C. Size and surface effects of silicon nanocrystals in graphene aerogel compoiste anodes for lithium ion batteries. Chem. Mater. 2018, 30, 7782–7792.

48. Jiang, L.; Lin, B.; Li, X.; Song, X.; Xia, H.; Li, L.; Zeng, H. Monolayer MoS2-Graphene Hybrid Aerogels with Controllable Porosity for Lithium-Ion Batteries with High Reversible Capacity. ACS Appl. Mater. Interfaces 2016, 8, 2680–2687.

49. Zhang, X.; Lin, Z.; Chen, B.; Zhang, W.; Sharma, S.; Gu, W.; Deng, Y. Solid-state flexible polyaniline/silver cellulose nanofibrils aerogel supercapacitors. J. Power Sources 2014, 246, 283–289.

50. Conway, B.E. Transition from “Supercapacitor” to “Battery” Behavior in Electrochemical Energy Storage. J. Electrochem. Soc. 1991, 138, 1539–1548.

51. Yang, F.; Xu, M.; Bao, S.-J.; Wei, H.; Chai, H. Self-assembled hierarchical graphene/polyaniline hybrid aerogels for electrochemical capacitive energy storage. Electrochim. Acta 2014, 137, 381–387.

52. Van Hoa, N.; Quyen, T.T.H.; Van Hieu, N.; Ngoc, T.Q.; Thinh, P.V.; Dat, P.A.; Nguyen, H.T.T. Three-dimensional reduced graphene oxide-grafted polyaniline aerogel as an active material for high performance supercapacitors. Synth. Met. 2017, 223, 192–198.

53. Han, S.; Wu, D.; Li, S.; Zhang, F.; Feng, X. Porous graphene materials for advanced electrochemical energy storage and conversion devices. Adv. Mater. 2014, 26, 849–864.

54. Mao, J.; Iocozzia, J.; Huang, J.; Meng, K.; Lai, Y.; Lin, Z. Graphene aerogels for efficient energy storage and conversion. Energy Environ. Sci. 2018, 11, 772–799.

55. Yang, Z.; Tian, J.; Yin, Z.; Cui, C.; Qian, W.; Wei, F. Carbon nanotube- and graphene-based nanomaterials and applications in high-voltage supercapacitor: A review. Carbon N. Y. 2019, 141, 467–480.

56. Borenstein, A.; Hanna, O.; Attias, R.; Luski, S.; Brousse, T.; Aurbach, D. Carbon-based composite materials for supercapacitor electrodes: A review. J. Mater. Chem. A 2017, 5, 12653–12672.

57. Hong, J.Y.; Bak, B.M.; Wie, J.J.; Kong, J.; Park, H.S. Reversibly compressible, highly elastic, and durable graphene aerogels for energy storage devices under limiting conditions. Adv. Funct. Mater. 2015, 25, 1053–1062.

58. Yu, M.; Han, Y.; Li, J.; Wang, L. Magnetic N-doped carbon aerogel from sodium carboxymethyl cellulose/collagen composite aerogel for dye adsorption and electrochemical supercapacitor. Int. J. Biol. Macromol. 2018, 115, 185–193.

59. Yang, X.; Shi, K.; Zhitomirsky, I.; Cranston, E.D. Cellulose Nanocrystal Aerogels as Universal 3D Lightweight Substrates for Supercapacitor Materials. Adv. Mater. 2015, 27, 6104–6109.

60. Yang, X.; Fei, B.; Ma, J.; Liu, X.; Yang, S.; Tian, G.; Jiang, Z. Porous nanoplatelets wrapped carbon aerogels by pyrolysis of regenerated bamboo cellulose aerogels as supercapacitor electrodes. Carbohydr. Polym. 2018, 180, 385–392.

61. Salgado, M.; Santos, F.; Rodríguez-Rojo, S.; Reis, R.L.; Duarte, A.R.C.; Cocero, M.J. Development of barley and yeast β-glucan aerogels for drug delivery by supercritical fluids. J. CO2 Util. 2017, 22, 262–269.

62. Mallepally, R.R.; Marin, M.A.; Surampudi, V.; Subia, B.; Rao, R.R.; Kundu, S.C.; McHugh, M.A. Silk fibroin aerogels: Potential scaffolds for tissue engineering applications. Biomed. Mater. 2015, 10, 035002.

63. Weng, L.; Boda, S.K.; Wang, H.; Teusink, M.J.; Shuler, F.D.; Xie, J. Novel 3D Hybrid Nanofiber Aerogels Coupled with BMP-2 Peptides for Cranial Bone Regeneration. Adv. Healthc. Mater. 2018, 7, 1–16.

64. Jia, H.; Tian, Q.; Xu, J.; Lu, L.; Ma, X.; Yu, Y. Aerogels prepared from polymeric β-cyclodextrin and graphene aerogels as a novel host-guest system for immobilization of antibodies: A voltammetric immunosensor for the tumor marker CA 15–3. Microchim. Acta 2018, 185, 517.

65. Shao, L.; Cao, Y.; Li, Z.; Hu, W.; Li, S.; Lu, L. Dual responsive aerogel made from thermo/pH sensitive graft copolymer alginate-g-P(NIPAM-co-NHMAM) for drug controlled release. Int. J. Biol. Macromol. 2018, 114, 1338–1344.
66. Mehling, T.; Smirnova, I.; Guenther, U.; Neubert, R.H.H. Polysaccharide-based aerogels as drug carriers. J. Non-Cryst. Solids 2009, 355, 2472–2479.